Supporting Information

Sukdeb Saha,[a] Prasenjit Mahato,[a] Mithu Baidya,[b] Sudip K. Ghosh,[b]* and Amitava Das[a]*

[a]CSIR-Central Salt and Marine Chemicals Research Institute, Bhavnagar, Gujarat-364002, India.

[b]Department of Biotechnology, Indian Institute of Technology, Kharagpur, West Bengal-721302, India.

Contents Page No.

Saha et. al., ChemComm. DOI: 10.1039/c2cc34490d [Supporting Information]

Synthetic methodology for L_1:

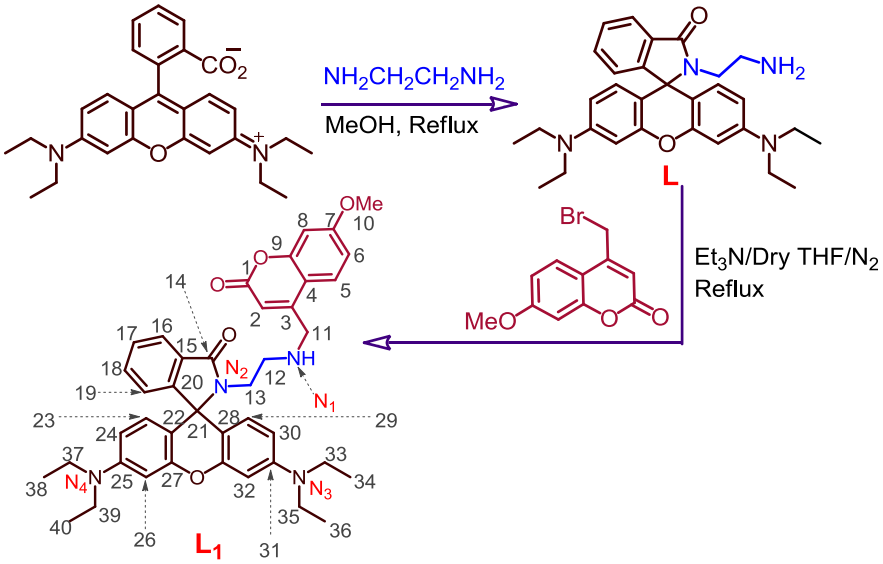

Amino ethyl rhodamine (**L**) (200 mg, 0.413 mmole) was dissolved in 20 ml of dry Tetrahedrofuran (THF). To this, Et_3N (62µl, 0.454 mmole) was added and the resulting solution was kept under N_2 for 15 minutes. Then 4-bromomethyl-7-methoxy coumarin (111 mg, 0.413 mmole) was taken in 10 ml of dry THF and added into the stirring solution in drop wise fashion. It was kept under reflux condition with stirring for 10h until all the starting materials become consumed. After that, solvent was removed with rotary evaporator. Then it was dissolved in 20 ml of $CHCl_3$ and washed with 10 ml of water. The organic layer was collected and dried over anhydrous Na_2SO_4 before concentration. It was finally purified by column chromatography using silica gel as stationary phase and $CHCl_3$ as solvent to isolate an off-white solid **L_1** in pure form with 87% yield (yield was calculated based on the starting reagents). ^{1}H NMR (500 MHz, CD_3CN, $SiMe_4$, *J* (Hz), δ ppm): 7.811 (1H, m, H_{18}), 7.512-7.483 (3H, m, H_{17}, H_{19}, H_{20}), 6.991 (1H, t, J= 3.5Hz, H_7), 6.857 (1H, s, H_9), 6.837(1H, d, J = 1.5 Hz, H_6), 6.398 (1H, s, H_{27}), 6.380 (1H, s, H_{33}), 6.329 (1H, d, J = 2.5 Hz, $H_{30,24}$), 6.306 (1H, s, H_{31}), 6.286 (1H, s, H_{25}), 6.091 (1H, s, H_2) , 3.849 (3H, s, H_{11}), 3.55 (2H, s, H_{12}), 3.288 (8H, q, J= 7 Hz,$H_{31,\ 40,\ 34,\ 36}$), 3.208 (2H, t, J= 6Hz, H_{14}), 2.451 (2H, t, J=7 Hz, H_{13}), 1.069 (12H, t, J=7 Hz, $H_{35,36,39,41}$). ^{13}C NMR (500 MHz, CD_3CN, $SiMe_4$, δ ppm) : 167.637, 162.041, 160.458, 154.917, 154.139,153.417, 152.791, 148.437, 132.118, 130.710, 128.160, 128.011, 127.792, 123.017, 121.905, 116.900, 111.613, 111.218, 108.984, 107.789, 104.963, 100.355, 96.882, 64.166, 55.180, 47.924, 46.976, 39.247, 28.926, 11.358. ESI-MS (+ve mode, m/z): 673.36 ($M + H^+$), Calc. for $C_{41}H_{44}N_4O_5$ is 672.33.

Saha et. al., ChemComm. DOI: 10.1039/c2cc34490d [Supporting Information]

^{1}H NMR spectra of L_1 in CD_3CN:

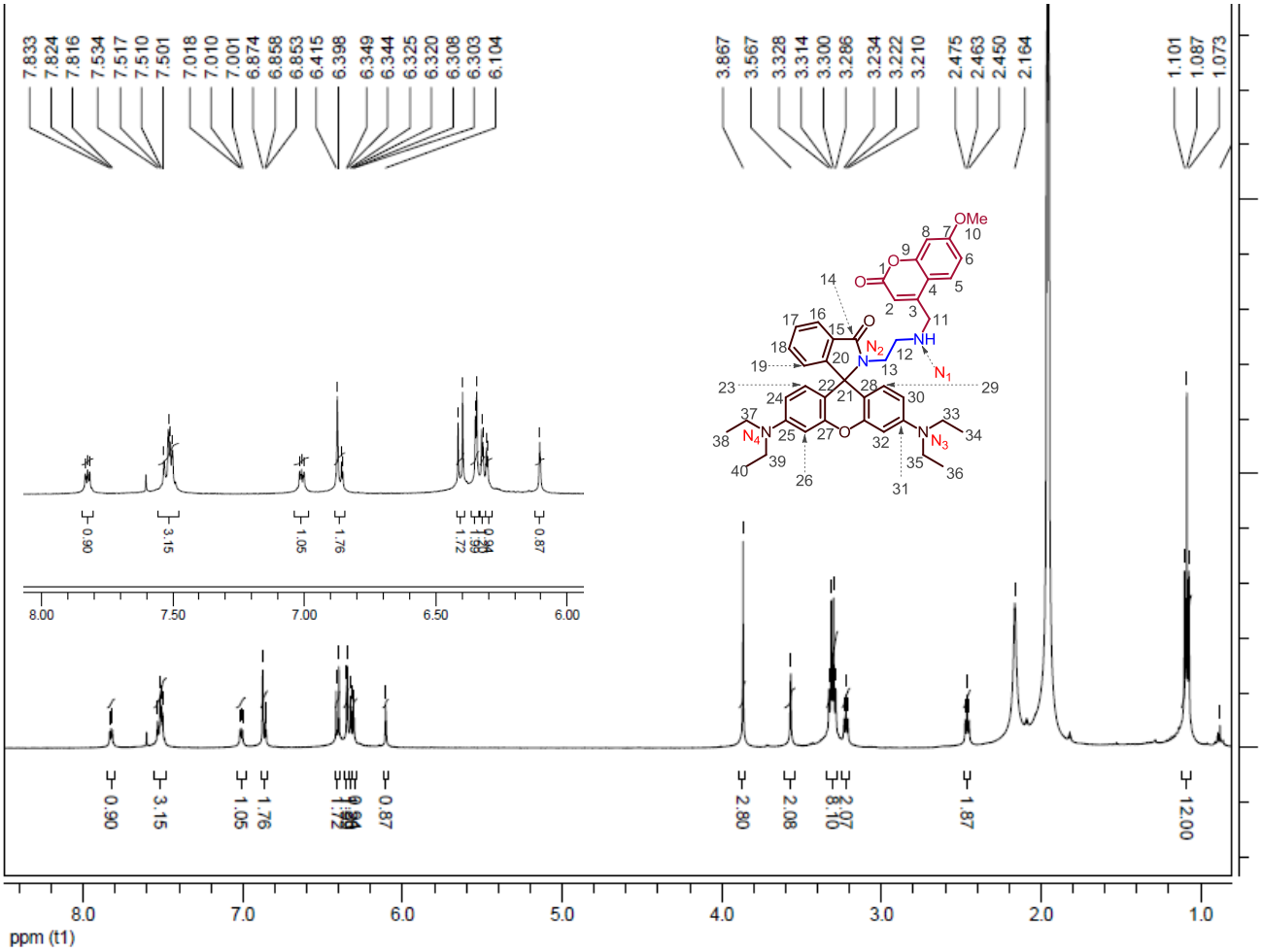

SI Figure 1: ^{1}H NMR of **L_1** in CD_3CN.

Saha et. al., ChemComm. DOI: 10.1039/c2cc34490d [Supporting Information]

^{13}C NMR spectra of L_1 in CD_3CN:

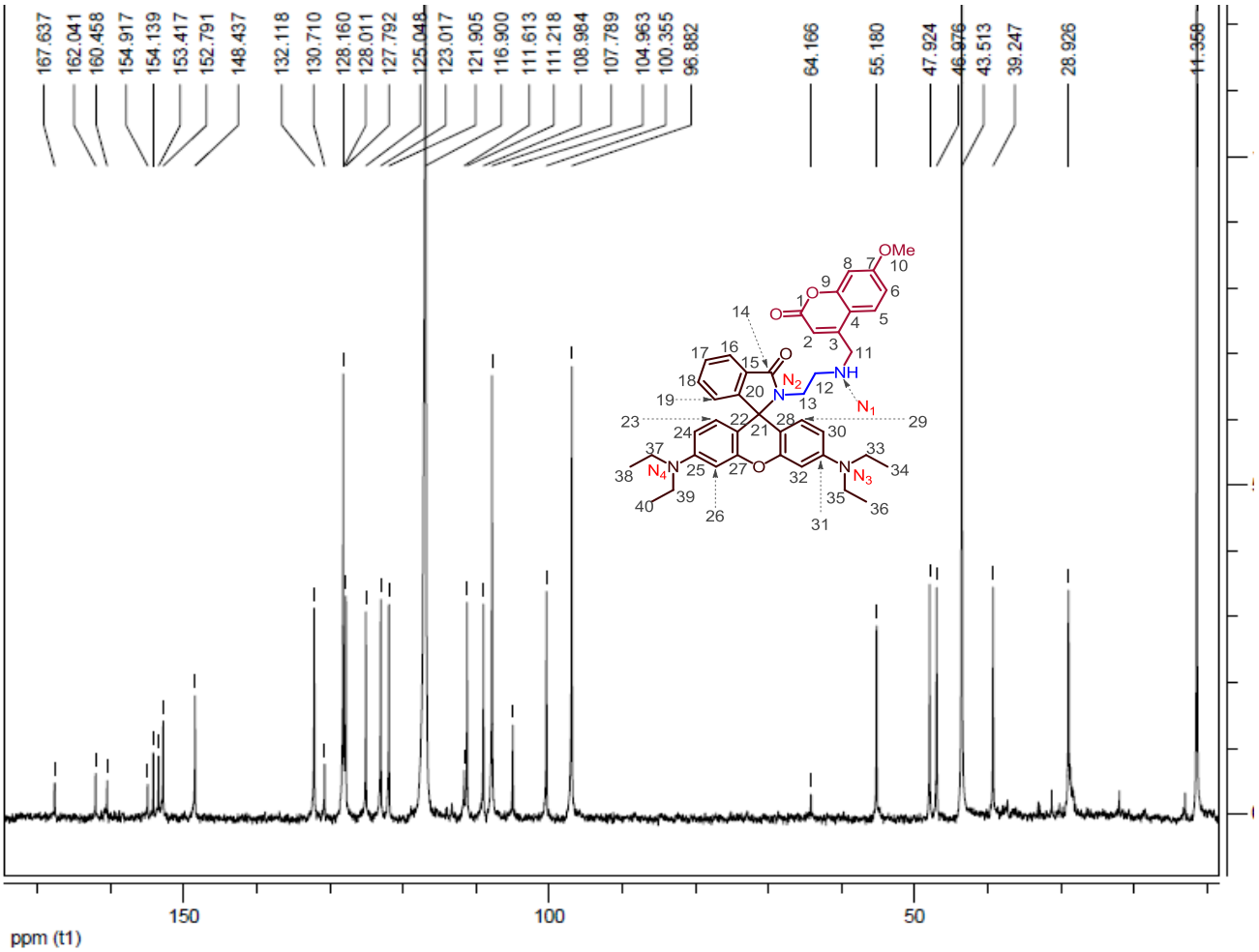

SI Figure 2: ^{13}C NMR spectra of **L_1** in CD_3CN.

Saha et. al., ChemComm. DOI: 10.1039/c2cc34490d [Supporting Information]

ESI-Ms spectra of L_1:

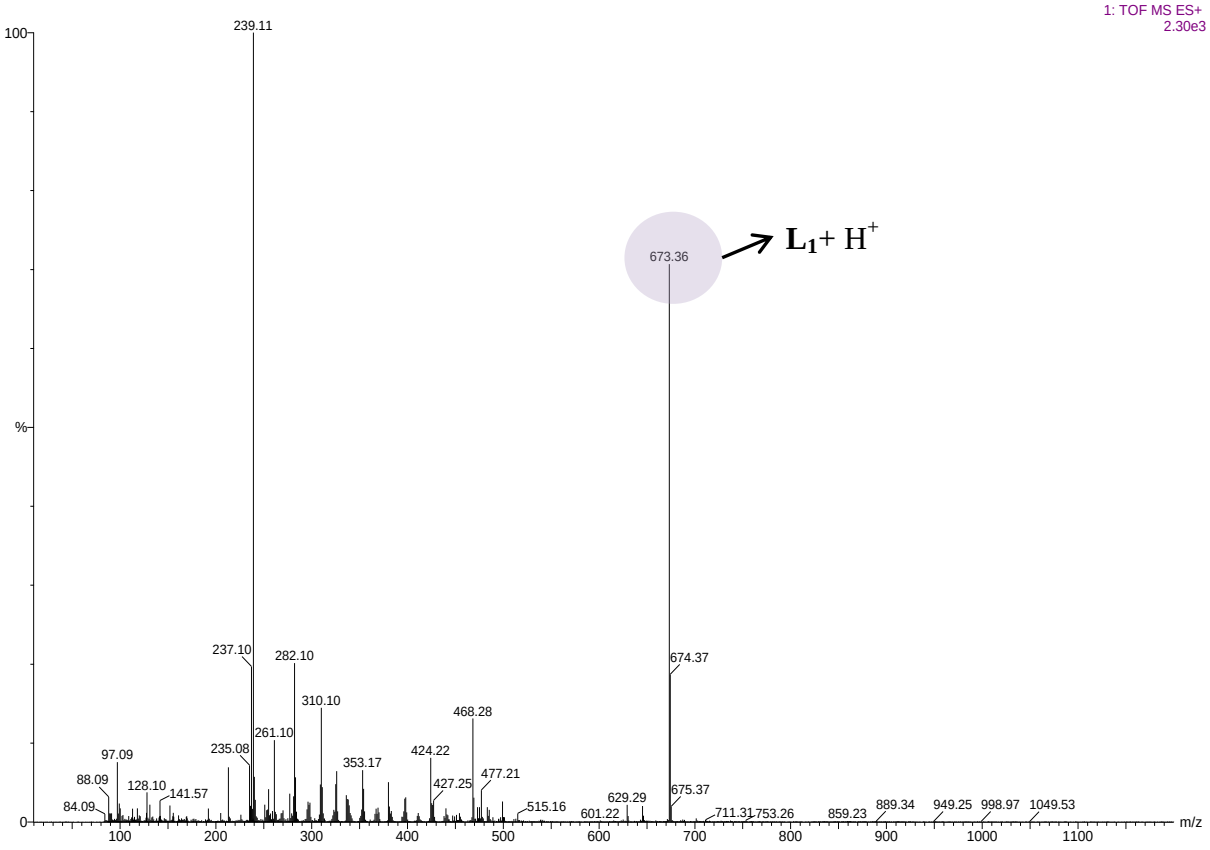

SI Figure 3: ESI-Ms spectra of L_1.

Saha et. al., ChemComm. DOI: 10.1039/c2cc34490d [Supporting Information]

FTIR Spectra of L_1:

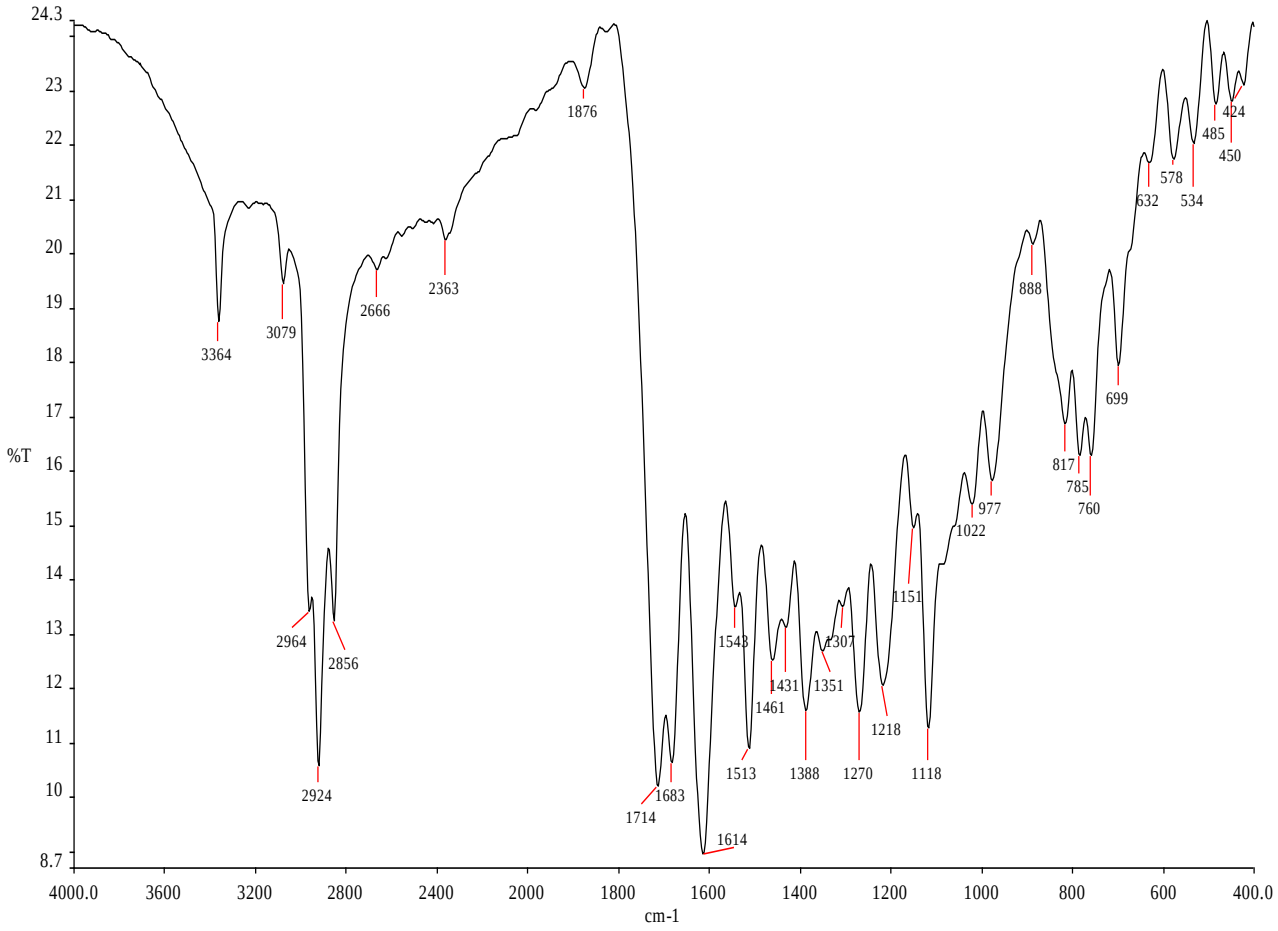

SI Figure 4: FTIR spectra of **L_1**.

Saha et. al., ChemComm. DOI: 10.1039/c2cc34490d [Supporting Information]

Synthetic methodology for the receptor 4-((benzylamino)methyl)-7-methoxy-2*H*-chromen-2-one L_2:

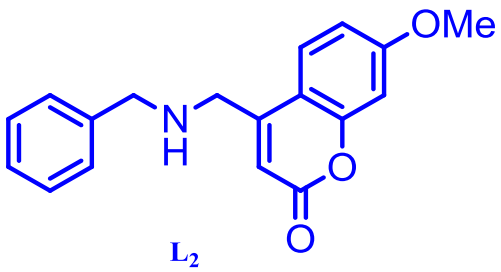

L_2

Benzyl amine (0.26 mmole) was dissolved in 5 ml of dry Tetrahedrofuran (THF). To this, Et_3N (28µl) was added and the resulting solution was kept under N_2 for 15 minutes. Then 4-bromomethyl-7-methoxy coumarine (66.2 mg, 0.26 mmole) was taken in another 5 ml of dry THF and added into the stirring solution in drop wise fashion. It was kept at reflux temperature under N_2 atmosphere with stirring for 10h until all the starting materials become consumed. After that, solvent was removed with rotary evaporator. Then it was dissolved in 10 ml of $CHCl_3$ and washed with 5ml of water. The organic layer was collected and dried over anhydrous Na_2SO_4 before concentration. It was finally purified by column chromatography using silica gel as stationary phase and MeOH: $CHCl_3$ (1:49) as solvent to isolate yellow solid **L_2** in pure form with 91% yield (yield was calculated based on the starting reagents). ^{1}H NMR (500 MHz,CD_3CN: $CDCl_3$,1:1, $SiMe_4$, *J* (Hz), δ ppm): 7.456 (1H, dd, J= 2.5 Hz), 7.380-7.320 (4H, m), 7.257 (1H, t, J= 7.5 Hz), 6.889-6.869 (3H), 6.337 (1H, s), 3.91 (2H), 3.861 (3H, s), 3.843 (2H, s). ^{13}C NMR(500 MHz, $CDCl_3$, δ ppm): 50.605, 55.361, 57.579, 102.850, 112.425, 114.164, 126.950, 129.226, 130.006, 130.433, 141.244, 155.474, 157.470, 163.333, 164.423. ESI-MS (+ve mode, m/z): 296.42 (M + H^+, 100%), Calc. for $C_{18}H_{17}NO_3$ is 295.33.

Saha et. al., ChemComm. DOI: 10.1039/c2cc34490d [Supporting Information]

^{1}H NMR spectra of L_2 in $CD_3CN/CDCl_3$:

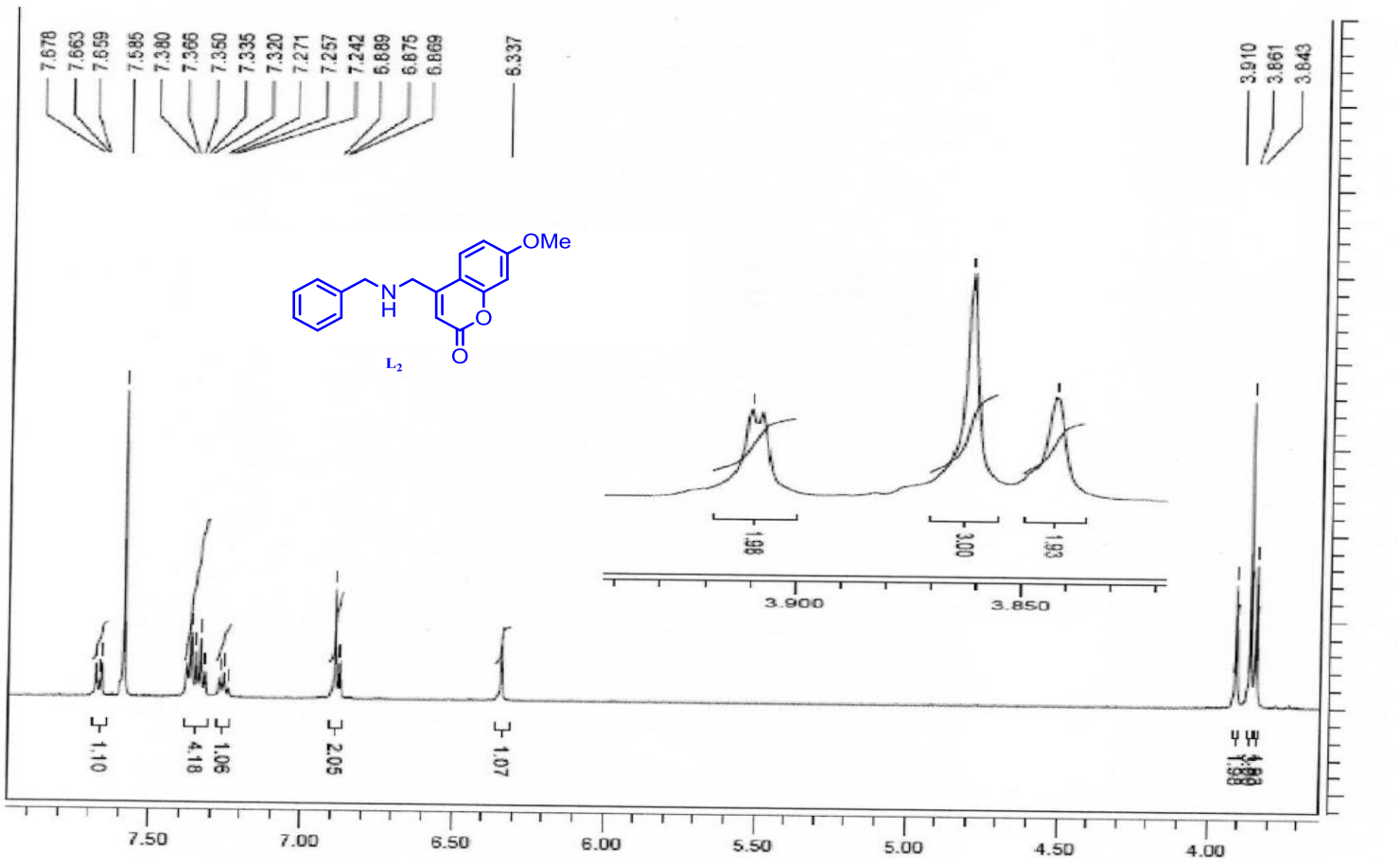

SI Figure 5: ^{1}H NMR of **L_2** in $CD_3CN/CDCl_3$ (1:1, v/v).

Saha et. al., ChemComm. DOI: 10.1039/c2cc34490d [Supporting Information]

^{13}C NMR spectra of L_3 in $CD_3CN/CDCl_3$:

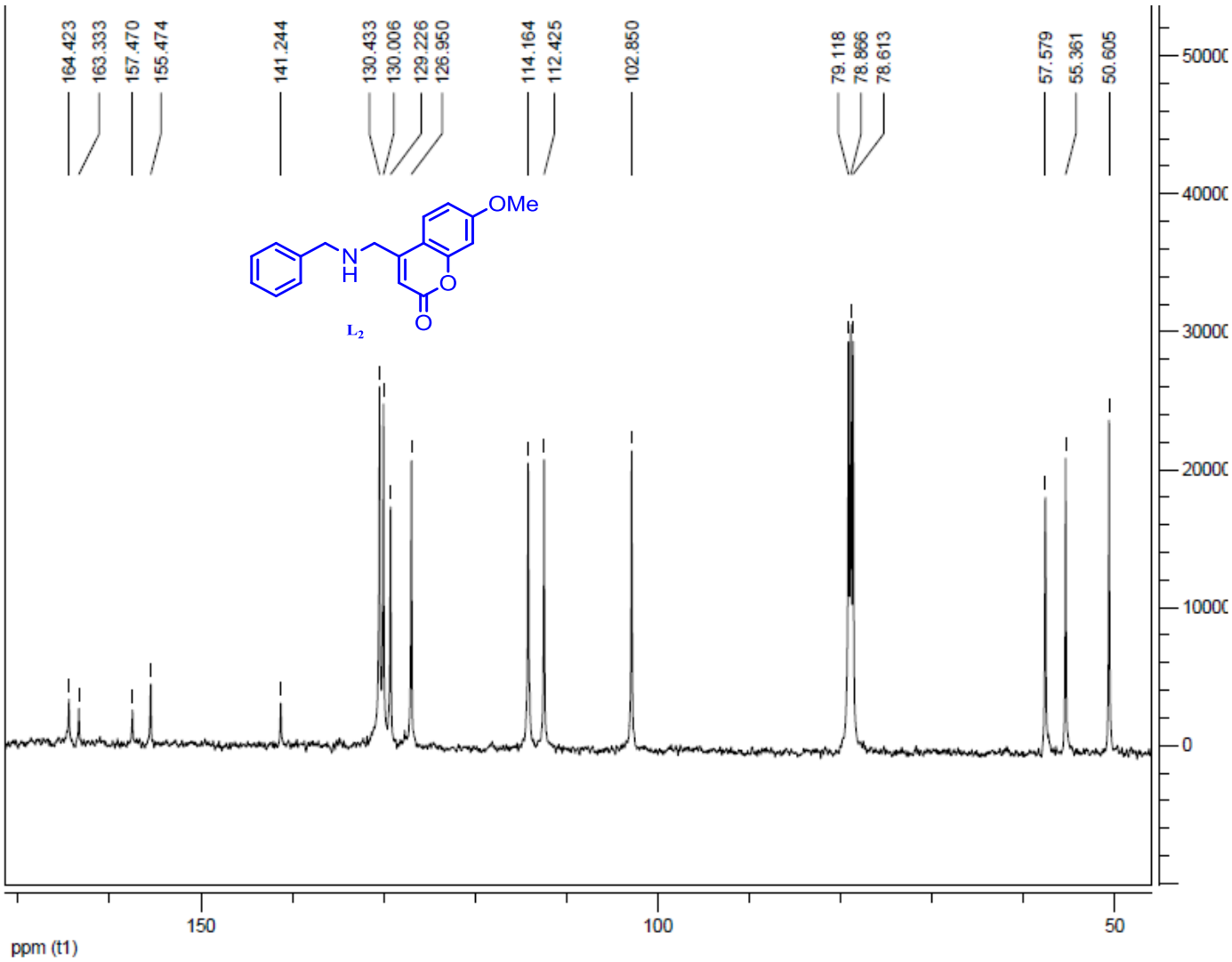

SI Figure 6: ^{13}C NMR of **L_2** in $CD_3CN/CDCl_3$ (1:1, v/v).

Saha et. al., ChemComm. DOI: 10.1039/c2cc34490d [Supporting Information]

ESI-Ms spectra of L_2.

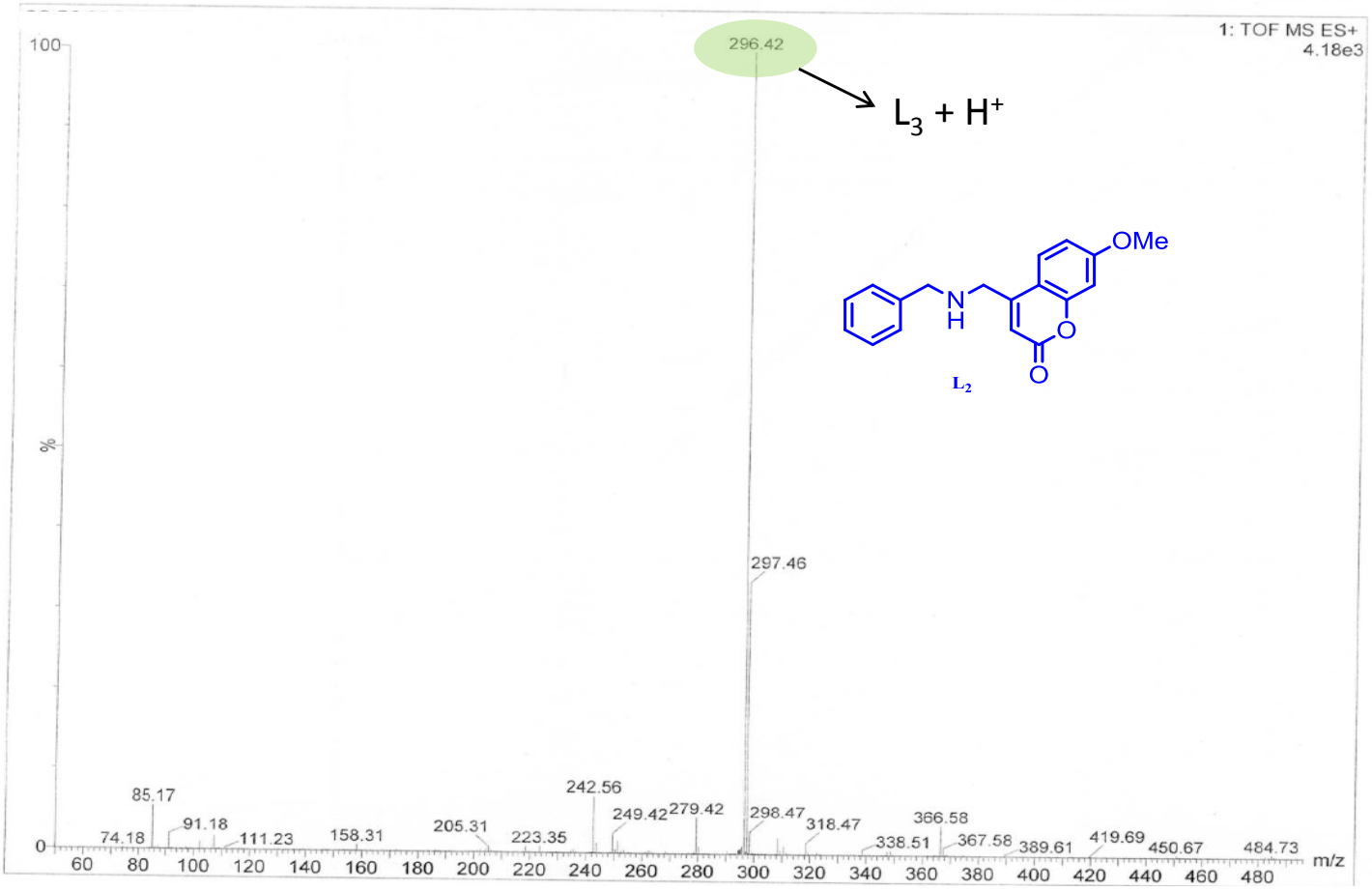

SI Figure 7: ESI-Ms spectra of L_2.

Saha et. al., ChemComm. DOI: 10.1039/c2cc34490d [Supporting Information]

^{13}C NMR of L_1 in absence and in presence of Hg^{2+} in $CDCl_3/CD_3CN$:

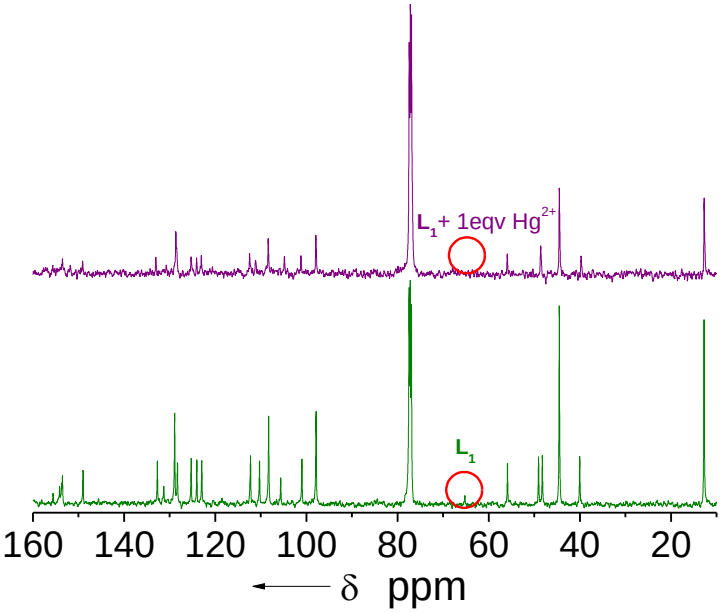

SI Figure 8: ^{13}C NMR of **L_1** in absence and in presence of Hg^{2+} in $CDCl_3/CD_3CN$.

Saha et. al., ChemComm. DOI: 10.1039/c2cc34490d [Supporting Information]

Beneshi-Hildebrand (B-H) plot obtained from the spectrophotometric titration of L_1 with Hg^{2+}:

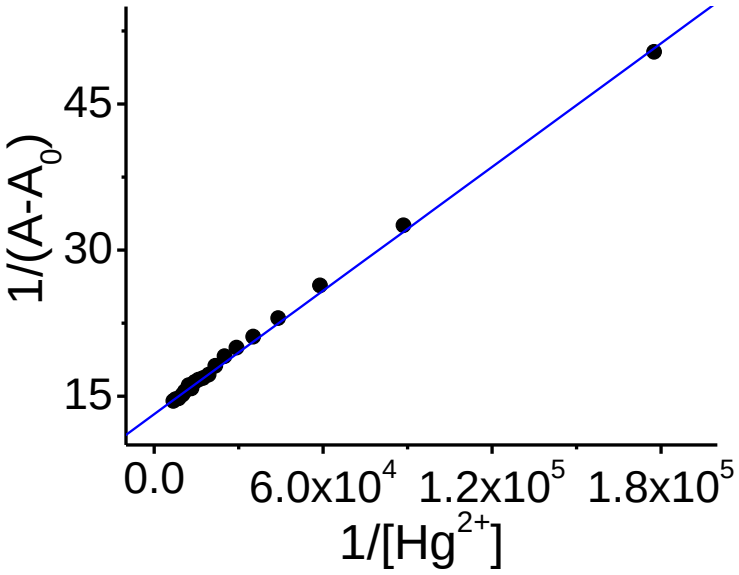

SI Figure 9: Beneshi-Hildebrand (B-H) plot obtained from the spectrophotometric titration of **L_1** with Hg^{2+} supported 1:1 binding stoichiometry (R^2=0.99723).

Saha et. al., ChemComm. DOI: 10.1039/c2cc34490d [Supporting Information]

Beneshi-Hildebrand (B-H) plot obtained from the emission titration of L_1 with Hg^{2+}:

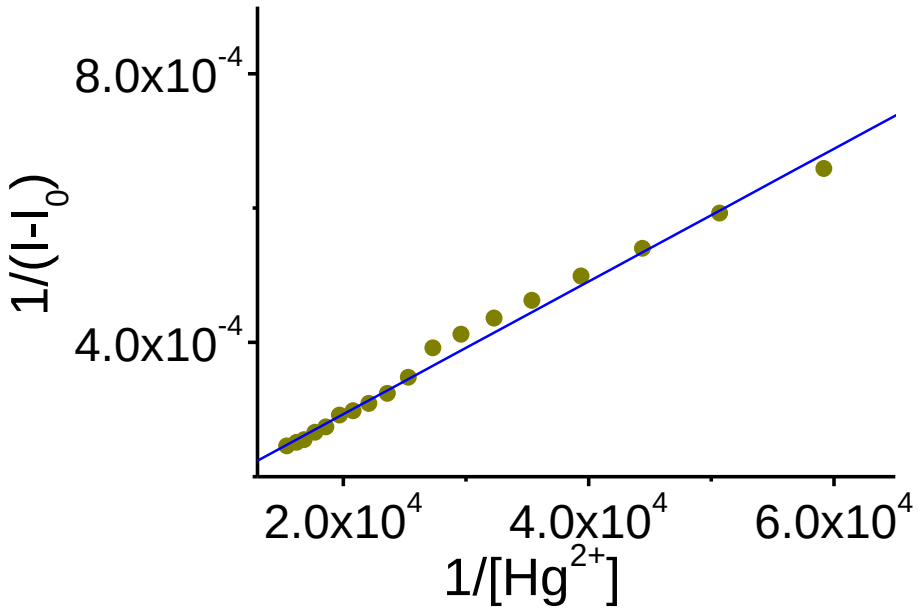

SI Figure 10: Beneshi-Hildebrand (B-H) plot obtained from the emission titration of **L_1** with Hg^{2+} supported 1:1 binding stoichiometry (R^2=0.994).

Saha et. al., ChemComm. DOI: 10.1039/c2cc34490d [Supporting Information]

Equation used for calculation of Energy transfer efficiency (ETE %):

$$\text{ETE \%} = \frac{\text{Quantum Yield of the acceptor fragment in the cassette excited at the donor}}{\text{Quantum Yield of the acceptor fragment in the cassette excited at the acceptor}} \times 100$$

Reference:

C. Thivierge, J. Han, R. M. Jenkins and K. Burgess, *J. Org. Chem.*, 2011, 76, 5219.

Saha et. al., ChemComm. DOI: 10.1039/c2cc34490d [Supporting Information]

ESI-Ms spectral evidence for the 1:1 adducts formation of L_1 with Hg^{2+}:

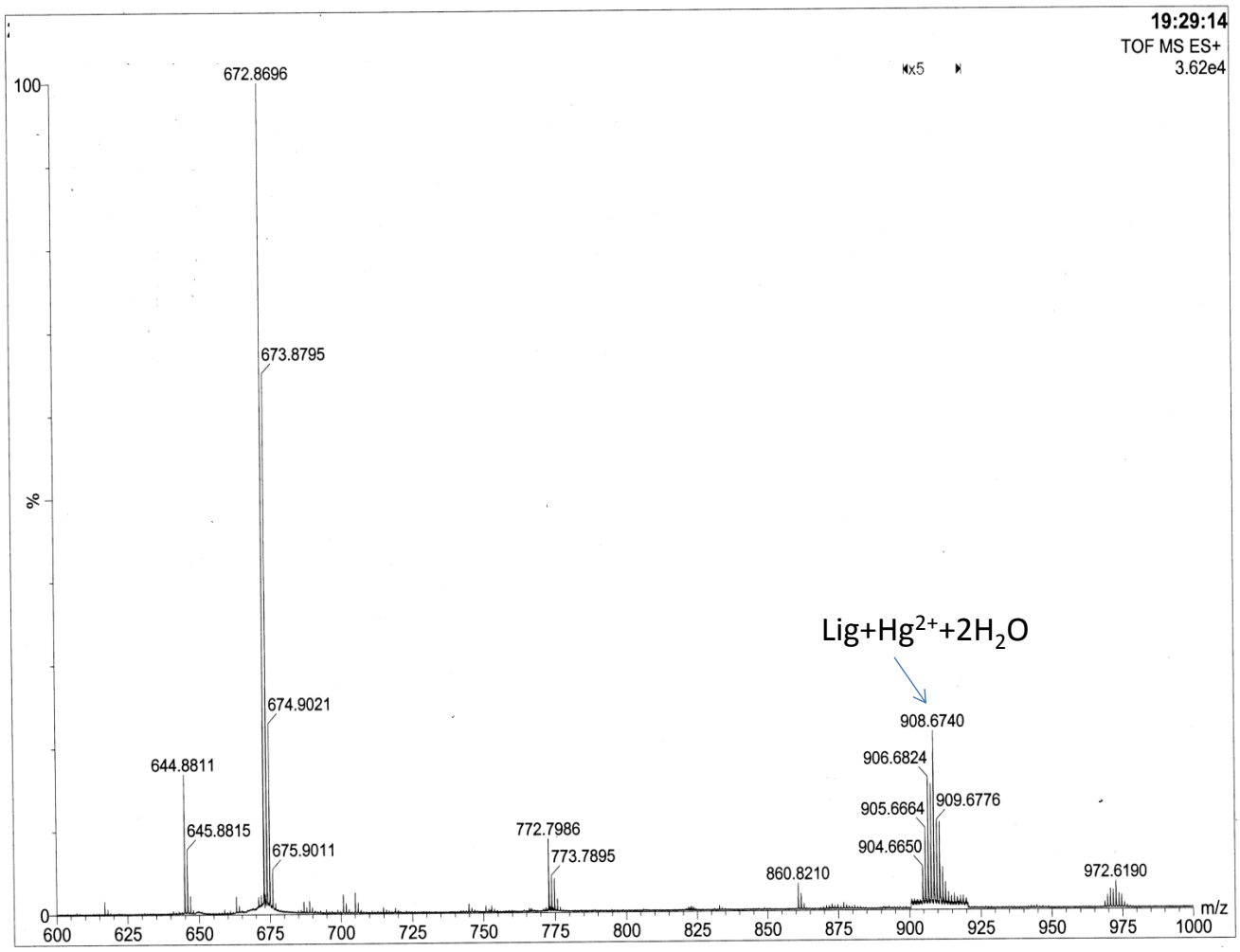

SI Figure 11: ESI-Ms spectral evidence for 1:1 adducts formation of L_1 with Hg^{2+}.

Saha et. al., ChemComm. DOI: 10.1039/c2cc34490d [Supporting Information]

Partial ^{1}H NMR titration of L_1 as a function of $Hg(ClO_4)_2$:

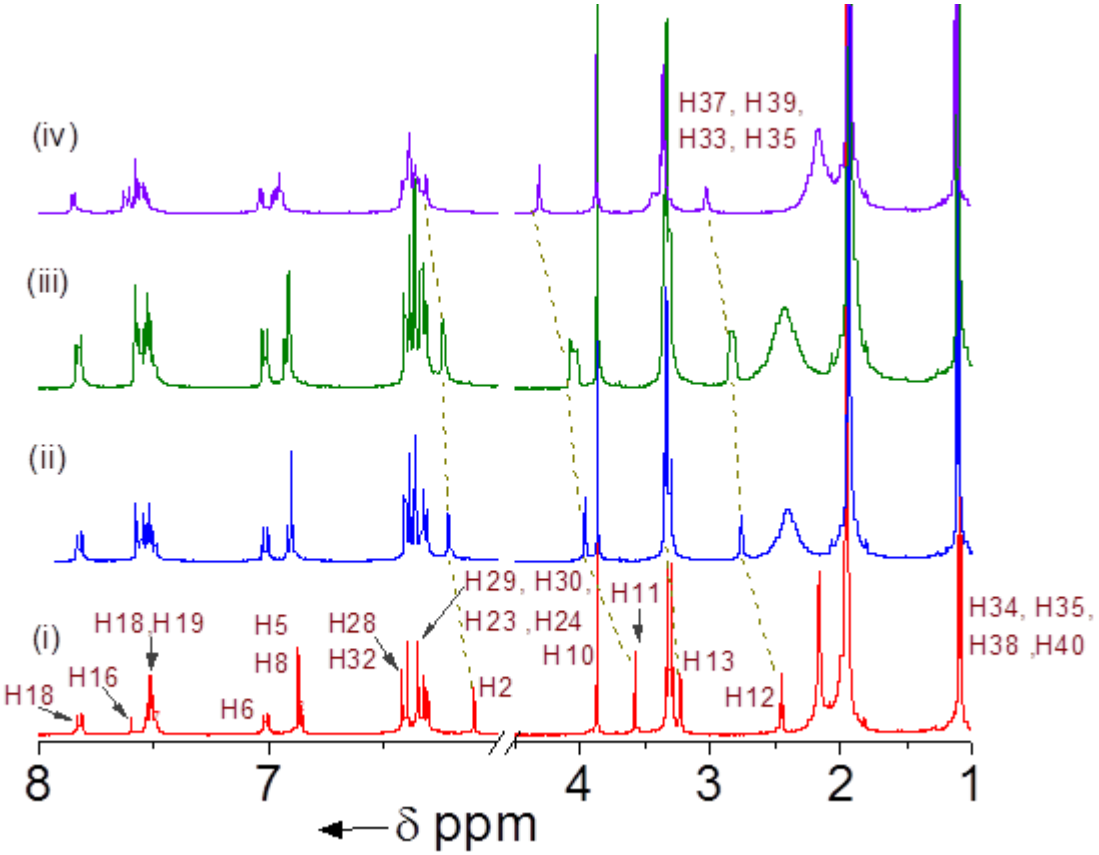

SI Figure 12: A plot of change in ^{1}H NMR spectral pattern for the receptor (i) $\mathbf{L_1}$; (ii) $\mathbf{L_1}$ with 0.5 eqv Hg^{2+}; (iii) $\mathbf{L_1}$ with 0.75 eqv Hg^{2+} and (iv) $\mathbf{L_1}$ with 1 eqv. Hg^{2+} in CD_3CN medium.

Saha et. al., ChemComm. DOI: 10.1039/c2cc34490d [Supporting Information]

Spectrophotometric interference study of L_1 with Hg^{2+} in presence of various metal ions:

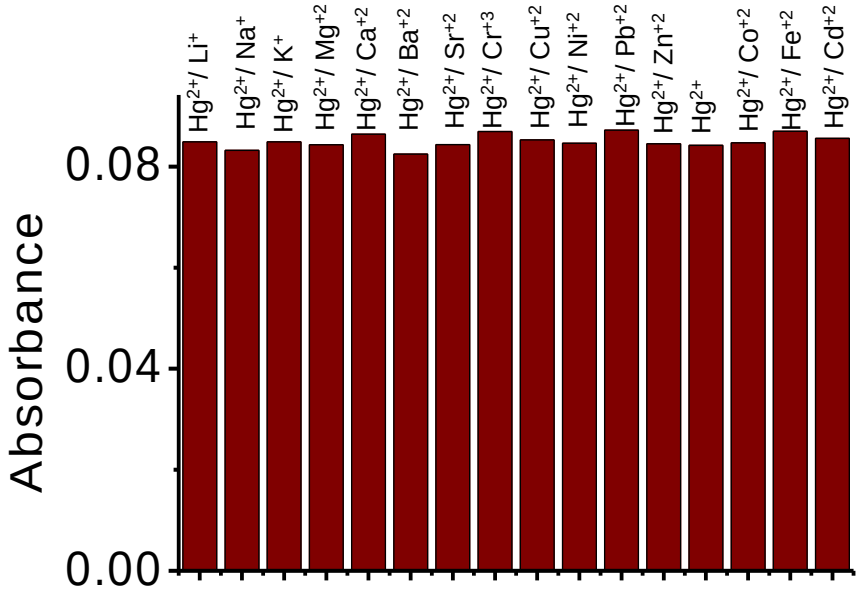

SI Figure 13: Spectrophotometric interference study of L_1(6.7×10^{-6} M) with Hg^{2+} (1.2×10^{-3} M) in presence of various metal ions (6.0×10^{-4} M) in MeOH/ HEPES buffer(1:1, v/v).

Saha et. al., ChemComm. DOI: 10.1039/c2cc34490d [Supporting Information]

Uv-Vis spectral studies for establishing the reversible binding of Hg^{2+} to the L_1:

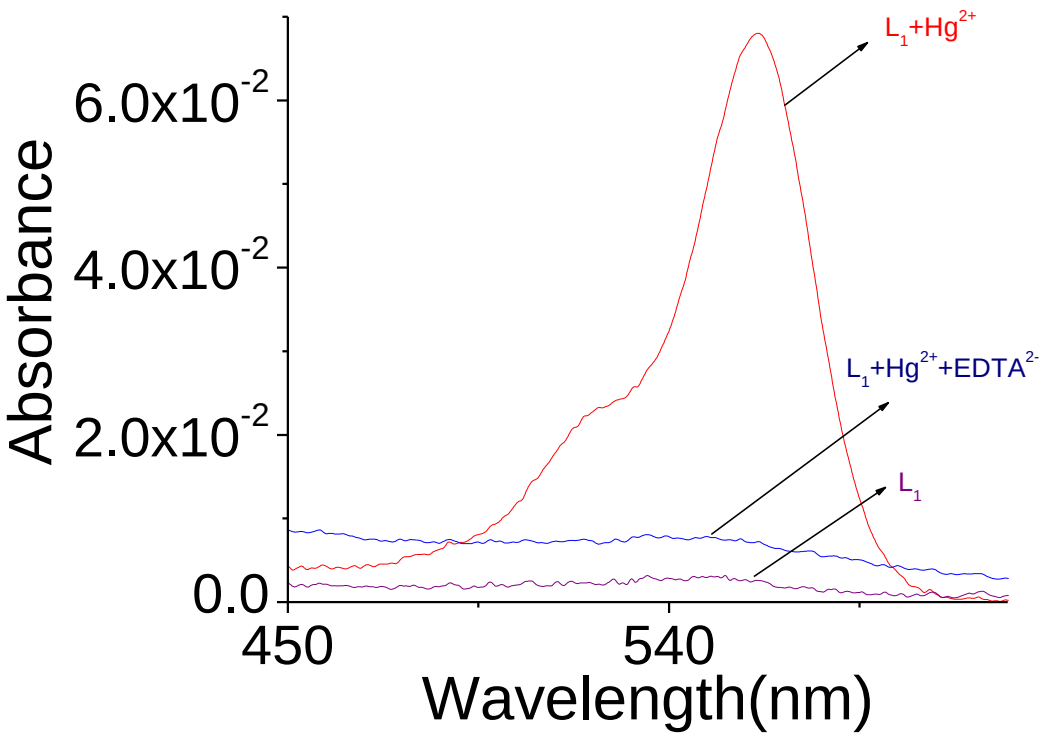

SI Figure 14: Uv-Vis studies for establishing the reversible binding of Hg^{2+} (1.53 x 10^{-4} M) to **L_1**(6.9 x 10^{-5} M) in presence of $EDTA^{2-}$(2 x 10^{-3} M) in MeOH-Water(1:1, v/v).

Saha et. al., ChemComm. DOI: 10.1039/c2cc34490d [Supporting Information]

Change of Emission intensity of L_1 at 585 nm as a function of the solution pH:

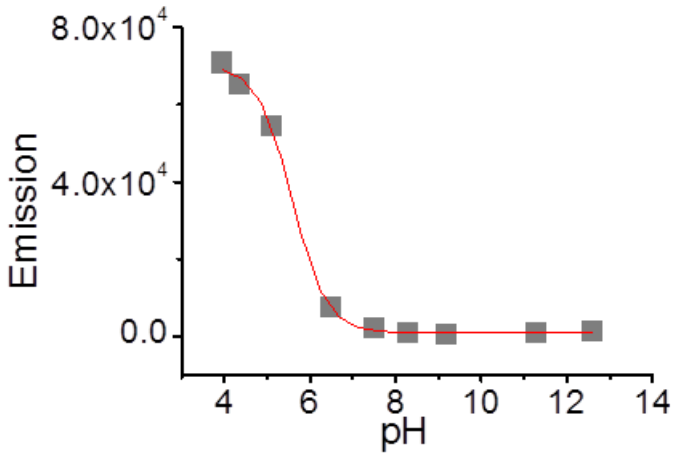

SI Figure 15: Change in emission intensity at 585 nm with variation in pH of the MeOH-water (1:1, v/v) solution for **L_1** (6.7×10^{-6} M).

Saha et. al., ChemComm. DOI: 10.1039/c2cc34490d [Supporting Information]

FTIR Spectra of L_1 in presence of 5 equivalent of $Hg(ClO_4)_2$:

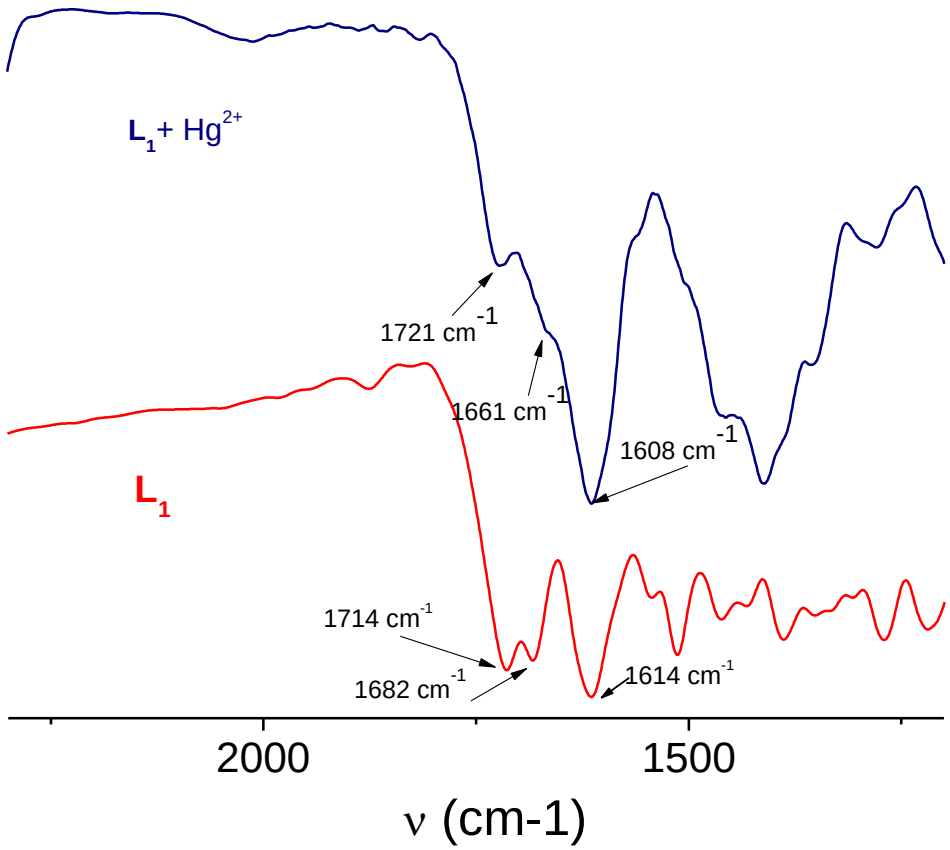

SI Figure 16: FTIR spectra of L_1 in presence of 5 equivalent of $Hg(ClO_4)_2$.

FTIR spectra have been recorded to understand the binding mode of Hg^{2+} with L_1 in presence of 5 mole equivalent of $Hg(ClO_4)_2$. In L_1, two carbonyl stretching were observed which are belong to coumarin C=O bond and amide carbonyl moiety from rhodamine unit. The peak appeared at the stretching frequency 1714 cm^{-1} could be appeared from coumarine moiety while peak at 1682 cm^{-1} could be appeared from amide carbonyl of rhodamine as amide stretching frequency should be lowered compared to the ester carbonyl frequency. The lowering of the stretching frequency of the amide carbonyl from 1682 cm^{-1} to 1661 cm^{-1} indicated definite coordination of Hg^{2+} to the amide C=O bond. However, a slight increment in the stretching frequency of the ester C=O was due to lowering of overall electron density on the coumarin moiety after coordination to metal ions thus no participation of ester C=O in Hg^{2+} coordination.

Saha et. al., ChemComm. DOI: 10.1039/c2cc34490d [Supporting Information]

Bar Diagram for changes in absorbance intensity for L_1 with metal ions:

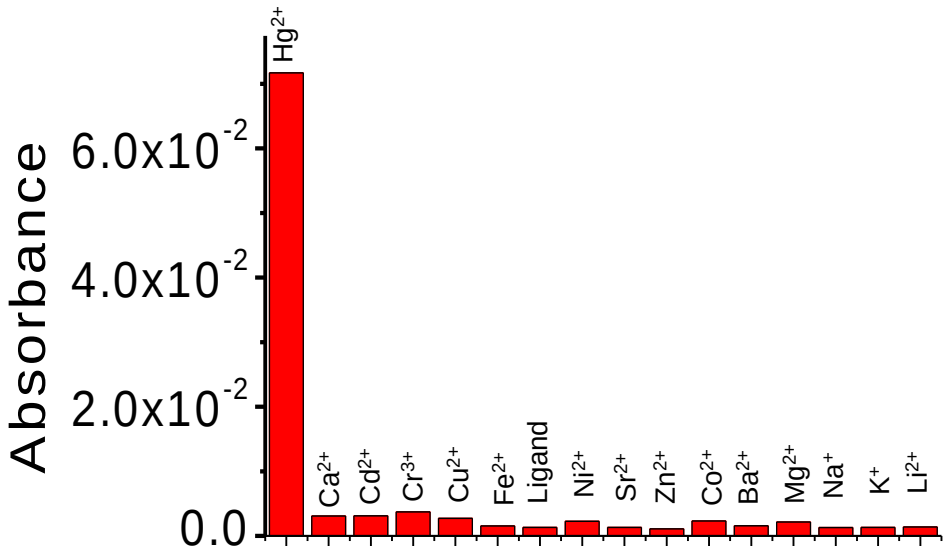

SI Figure 17: Bar diagram for the changes in absorbance intensity of **L_1**(6.7×10^{-6} M) with metal ions(1.0×10^{-4} M).

Saha et. al., ChemComm. DOI: 10.1039/c2cc34490d [Supporting Information]

Bar Diagram for changes in emission intensity for L_1 with metal ions:

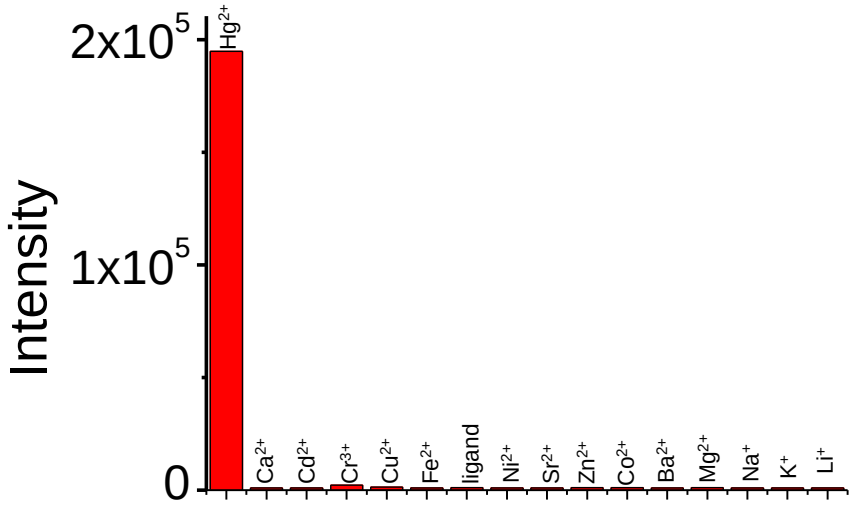

SI Figure 18: Bar diagram for the changes in absorbance intensity of **L_1**(6.7×10^{-6} M) with metal ions(1.5×10^{-4} M).

Saha et. al., ChemComm. DOI: 10.1039/c2cc34490d [Supporting Information]

Job's plot for L_1 with Hg^{2+} showing 1:1 stoichiometry:

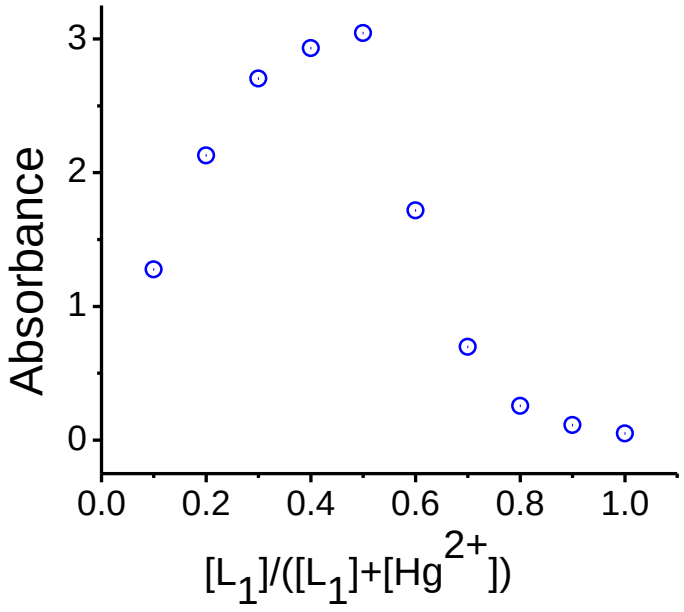

SI Figure 19: Job's plot between **L_1** and Hg^{2+} confirmed 1:1 adducts.

Saha et. al., ChemComm. DOI: 10.1039/c2cc34490d [Supporting Information]

Absorption spectra of L_1 in presence of Hg^{2+} at different pH:

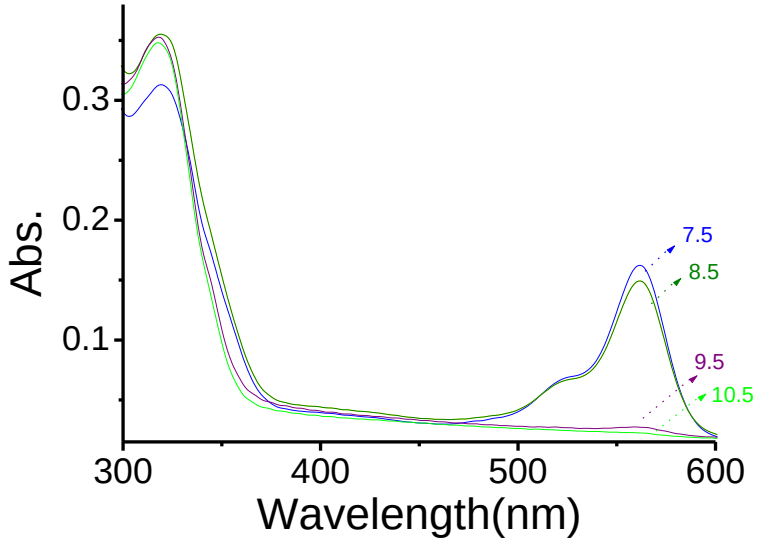

SI Figure 20: Absorption spectra for **L_1**(6.9×10^{-6} M) in presence of Hg^{2+}(1.0×10^{-4} M) at different basic pH.

Saha et. al., ChemComm. DOI: 10.1039/c2cc34490d [Supporting Information]

Emission spectra of L_1 in presence of Hg^{2+} at different pH:

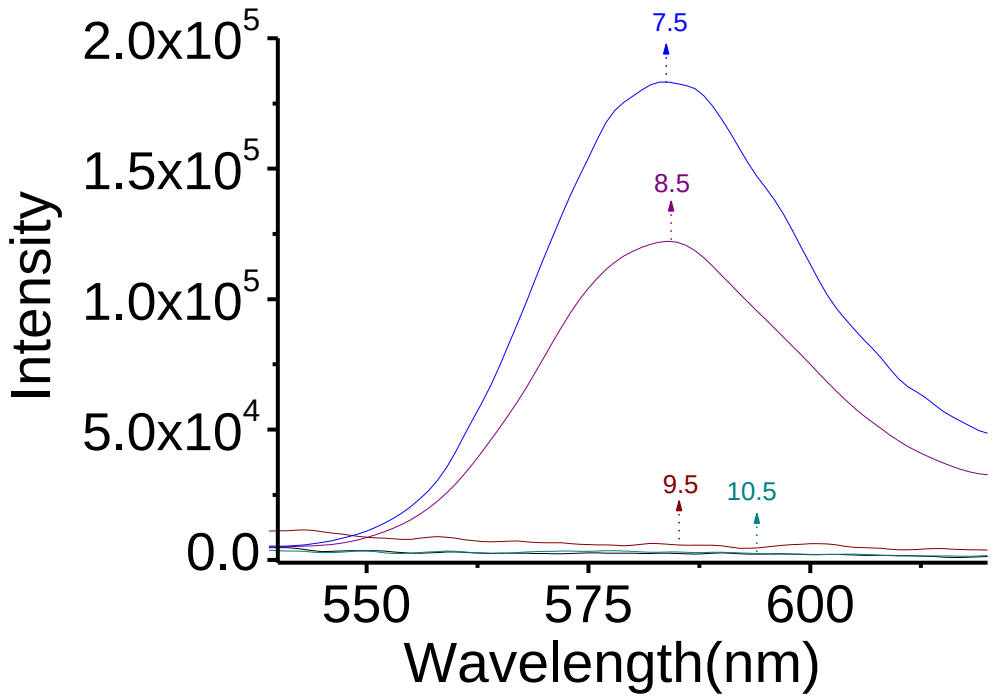

SI Figure 21: Emission spectra for **L_1** (6.9×10^{-5} M) in presence of Hg^{2+}(1.0×10^{-4} M) at different basic pH (λ_{Ext} 320 nm).

Saha et. al., ChemComm. DOI: 10.1039/c2cc34490d [Supporting Information]

Confocal microscopic images of L_1 in presence and in absence of Hg^{2+} in MCF7 cells:

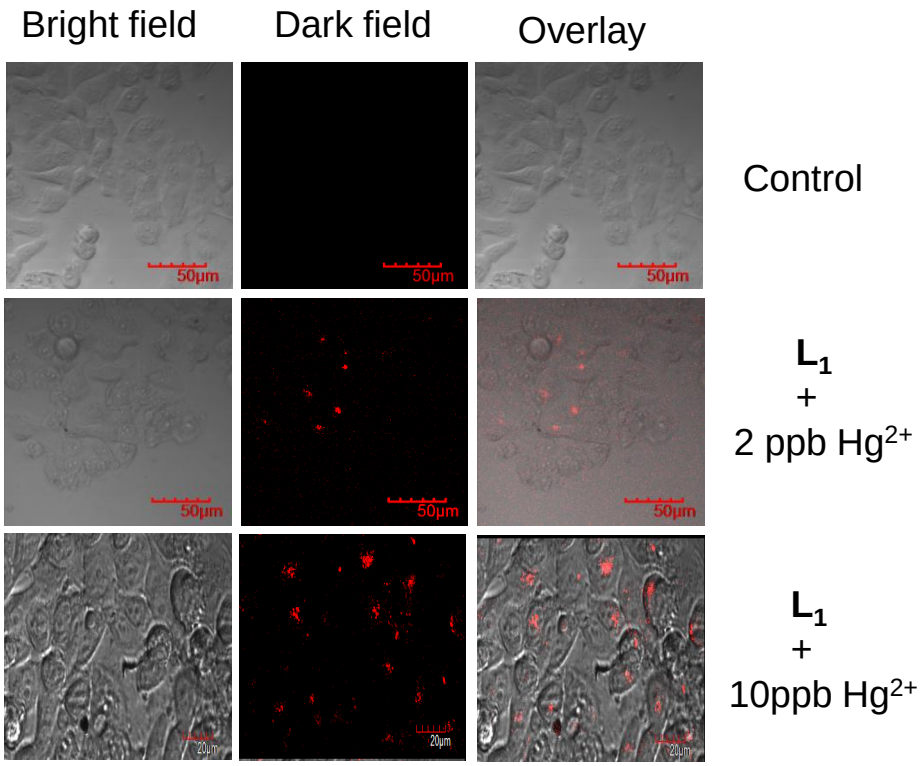

SI Figure 22: Confocal microscopic images of **L_1** (10 μM) in absence and in presence of Hg^{2+} (2-10ppb) in MCF7 cells (λ_{Ext} 543nm).

Saha et. al., ChemComm. DOI: 10.1039/c2cc34490d [Supporting Information]

Fluorescence microscopic images of L_1 in presence and in absence of Hg^{2+} in MCF7 cells:

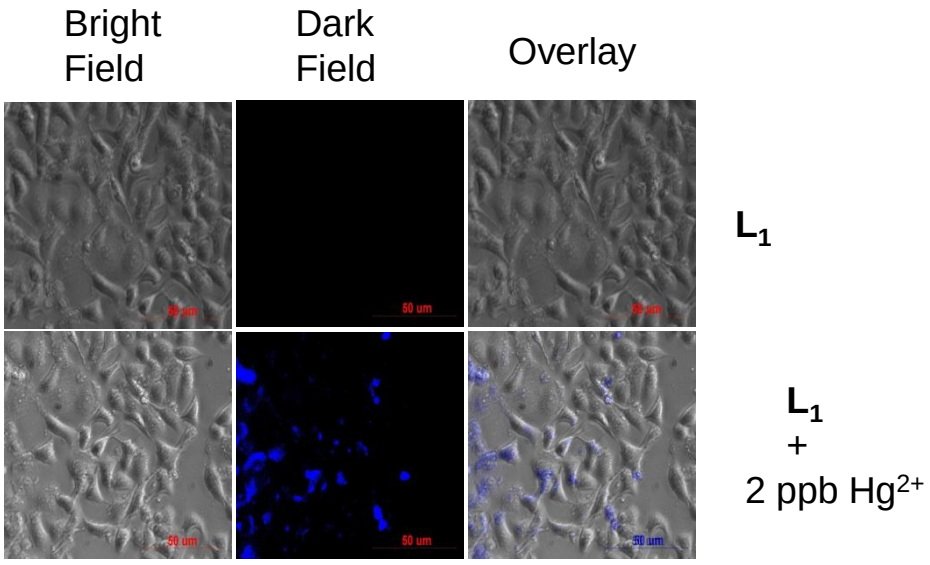

SI Figure 23: Fluorescence microscopic images of **L_1** (10 μM) in absence and in presence of Hg^{2+} (2ppb) in MCF7 cells (λ_{Ext} 330-385nm).

Saha et. al., ChemComm. DOI: 10.1039/c2cc34490d [Supporting Information]

Reversibility studies for binding of the reagent L_1 to Hg^{2+} present in the breast cancer cell (MCF7 cells) with subsequent treatment with KI:

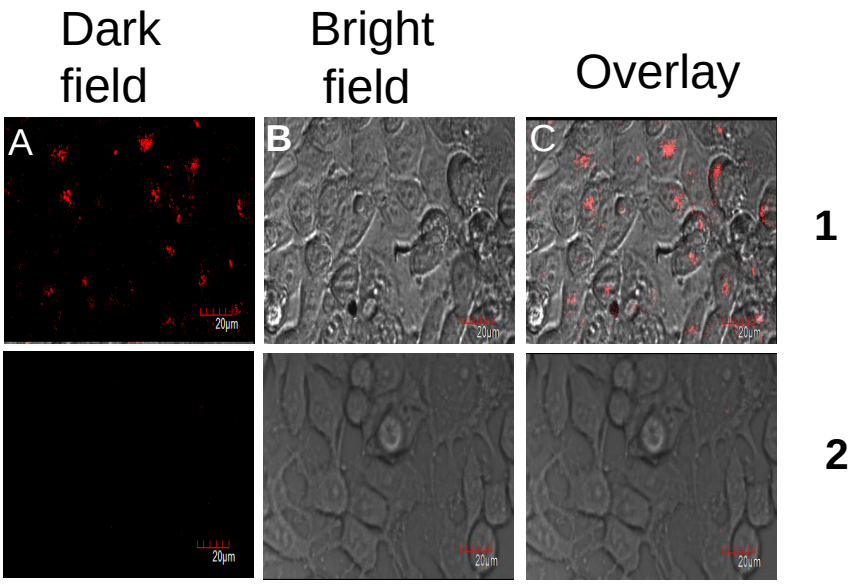

SI Figure 24: Confocal dark field (A),Bright field (B), and overlay images(C) of MCF7 cells. (1) The cells were supplemented with Hg^{2+} (10ppb) and then were stained with 10 μM of **L_1** for 1.0 H at 37°C, (2) with Hg^{2+}(10 ppb), 10 μM **L_1** and then KI(30 μM) in the growth media for 1.0 h at 37 °C (λ_{ext} = 543 nm).

MTT assay studies for evolution of cytotoxicity of the reagent L_1 towards the breast cancer cell (MCF7 cells):

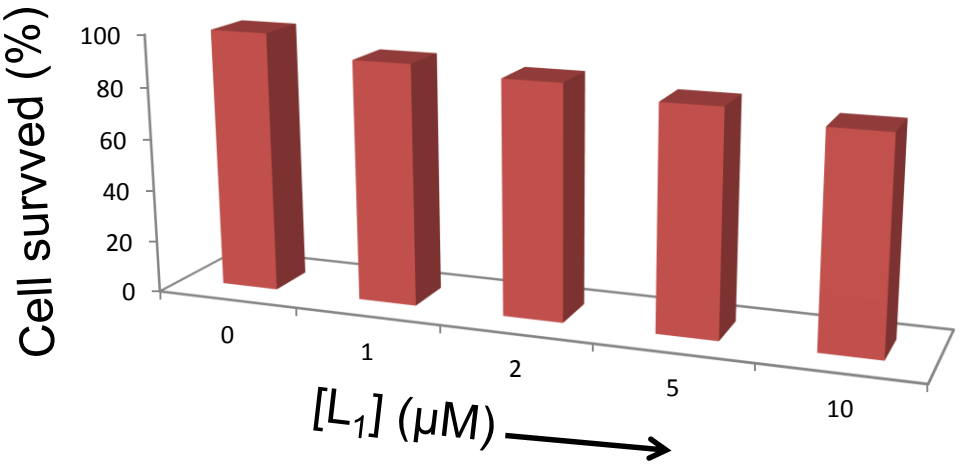

SI Figure 25: Check of viability of **L_1** on the breast cancer cells (MCF7 cells). Here % of viability was calculated with respect to the growth considering 100% without **L_1**.

Cell Cytotoxicity Assay

Cytotoxicity of **L_1** on MCF7 cells was determined by conventional MTT assay (*J. Natl. Cancer Inst.,* **1990,** *8,* 1113-1117). MCF7 cells in their exponential growth phase were trypsinised and seeded in 96-well flat-bottom culture plates at a density of 3 x 10^3 cells per well in 100 µl DMEM complete medium (Himedia, India). The cells were allowed to adhere and grow for 24 hr at 37 ºC in CO_2 incubator (New Brunswick Scientific, U.S.A.), and then the medium was replaced with 100 µl fresh incomplete medium containing various concentrations of **L_1** (0 to 10 µM). The assay was performed in quadruplet for each concentration. Cells were then incubated for 12h, after which the culture medium was removed, and 100 µl of 1 mg/ml MTT reagent in PBS was added to each well. Thereafter, it was incubated for 4 hrs; during this period active mitochondria of viable cells reduce MTT to purple formazan. Unreduced MTT were then discarded and DMSO (100 µl) was added into each well to dissolve the formazan precipitate, which was then measured spectrophotometrically using a microplate reader at 570 nm. The cytotoxic effect of each treatment was expressed as percentage of cell viability relative to the untreated control cells. [MTT= (3-(4, 5-Dimethylthiazol-2-yl)-2, 5-diphenyltetrazolium bromide, a yellow tetrazole].

Reference: L. V. Rubinstein, K. D. Paull, R. M. Simon, P. Skehan, D. A. Scudiero, A. Monks and M. R. Boyd, *J. Natl. Cancer Inst.*, 1990, **82**, 1113.